Supplementary Information (SI) for Nanoscale.
This journal is © The Royal Society of Chemistry 2024

Supplementary Information : Ultra-Low Noise Measurements of Ionic Transport Within Individual Single-Walled Carbon Nanotubes

Laure BSAWMAII[1], Clément DELACOU[1], Valerii KOTOK[1,2], Sébastien MEANCE[1], Koutayba SAADA[1], M. Amine KRIBECHE[1], Saïd TAHIR[1], Christophe ROBLIN[1], Antonin LOUISET[3], Hanako OKUNO[3], Manoel MANGHI[4], John PALMERI[1], François HENN[1], Adrien NOURY[1], and Vincent JOURDAIN[1,*]

[1]Laboratoire Charles Coulomb (L2C), Univ Montpellier, CNRS, Montpellier, France
[2]Ukrainian State University of Chemical Technology, 8, Gagarin ave. 49005 Dnipro
[3]Univ. Grenoble Alpes, CEA, IRIG-MEM, 38000, Grenoble, France
[4]Laboratoire de Physique Théorique (LPT UMR 5152), Université Toulouse III - Paul Sabatier, CNRS, 31062 Toulouse, France
[*]vincent.jourdain@umontpellier.fr

ABSTRACT

This supplement provides additional data on:
- ionic conductance versus KCl concentration for different devices,
- influence of IPA rinsing and plasma cleaning on ionic conductance (CNT and control),
- reversal potential data processing and modeling (Nernst approach),
- comparison between PSD and LPSD spectra,
- LPSD spectra at different applied voltages (CNT, control, leaky device without CNT),
- evolution of A_H with I^2,
- Raman and TEM data.

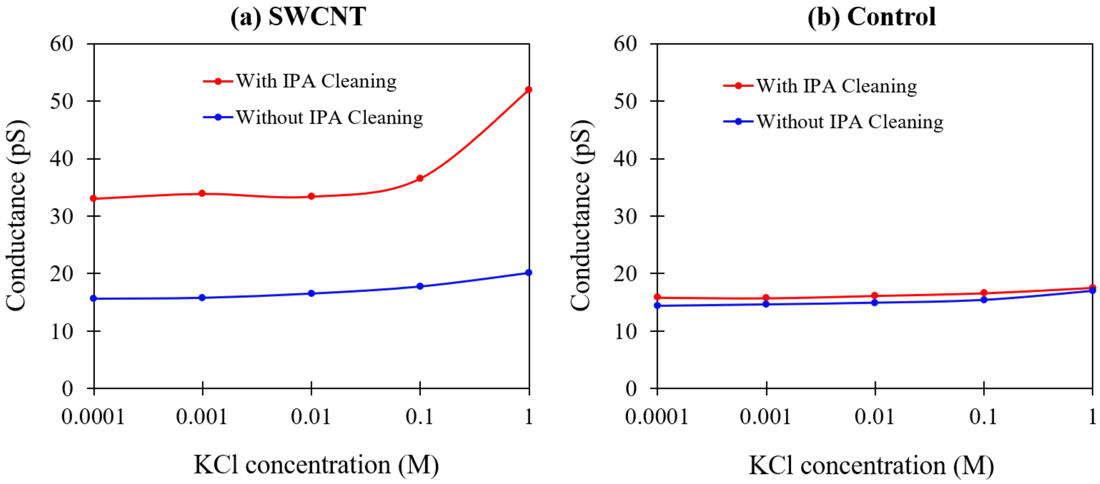

Figure S 1. Conductance measurements for different KCl concentrations for a second device on quartz substrate (device Q2), in case of (a) nanotube and (b) control parts. The blue and red curves correspond, respectively, to the measurements before and after IPA cleaning. On the nanotube side, the conductance increases after IPA rinsing, contrary to the control side. These results show that an appropriate IPA rinsing can help to unplugging the nanotube ends without creating leaks in the device. Details of the IPA cleaning procedure are given in the materials and methods section.

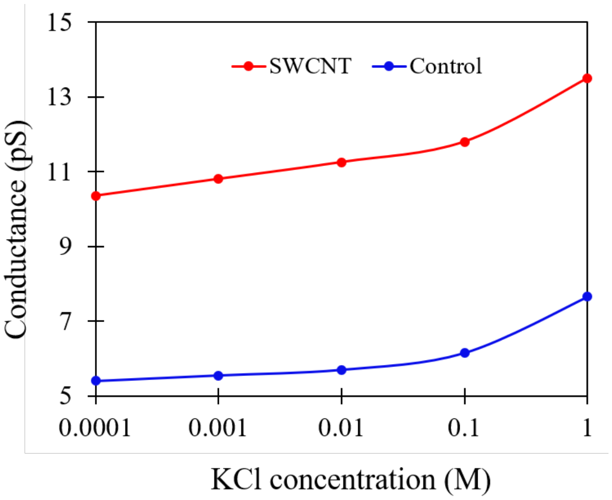

Figure S 2. Ionic conductance measurements for a third device on quartz substrate (device Q3) after IPA cleaning, for different KCl concentrations. On the nanotube side (red points), the conductance increased by a factor of two after IPA cleaning (from 5.2 to 10.4 pS in MQ water, not shown here), contrary to the control side (blue points) where it remained unchanged after IPA rinsing.

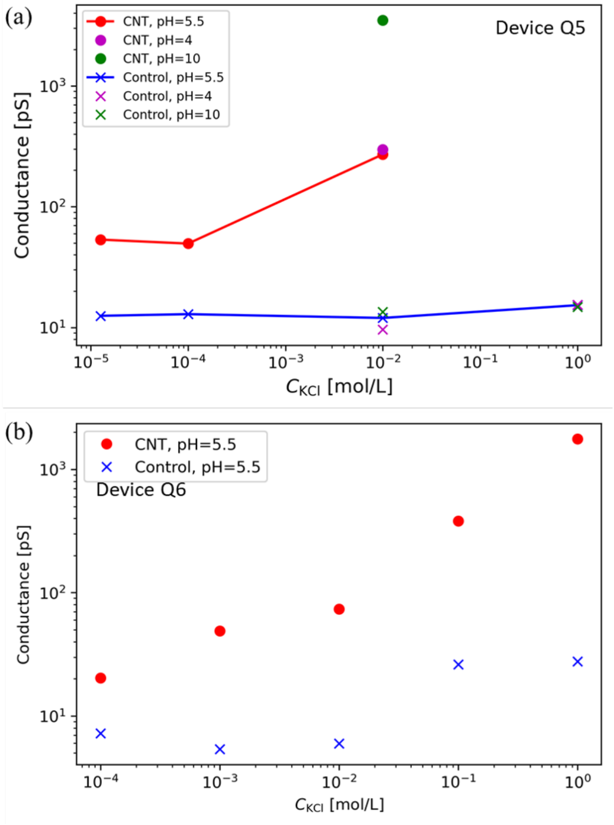

Figure S 3. Ionic conductance versus KCl concentration for two devices on quartz substrate with fabrication including the plasma cleaning step: (a) device Q5, (b) device Q6. In each case, the data for the CNT and control sides are shown. In this case, IPA rinsing was not needed to induce ionic transport on the nanotube side.

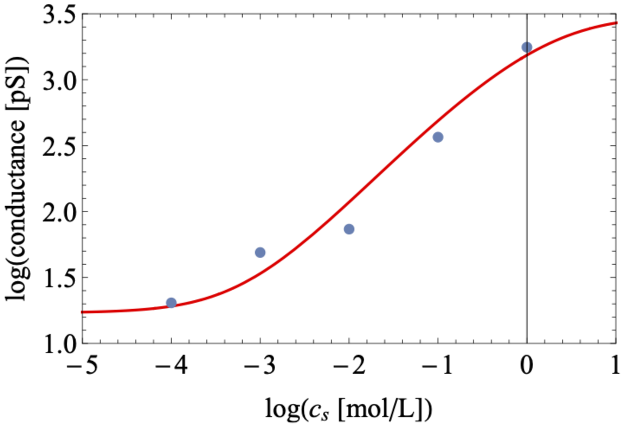

Figure S 4. Theoretical modeling of ionic conductance versus KCl concentration for device Q6. A good fit is obtained with the following parameter values: $R = 0.7$ nm, $b = 262$ nm, $\sigma_f = 0.023$ C/m, $\sigma_0 = 0.288$ C/m^2 and $p\mathrm{K} = 7.13$.

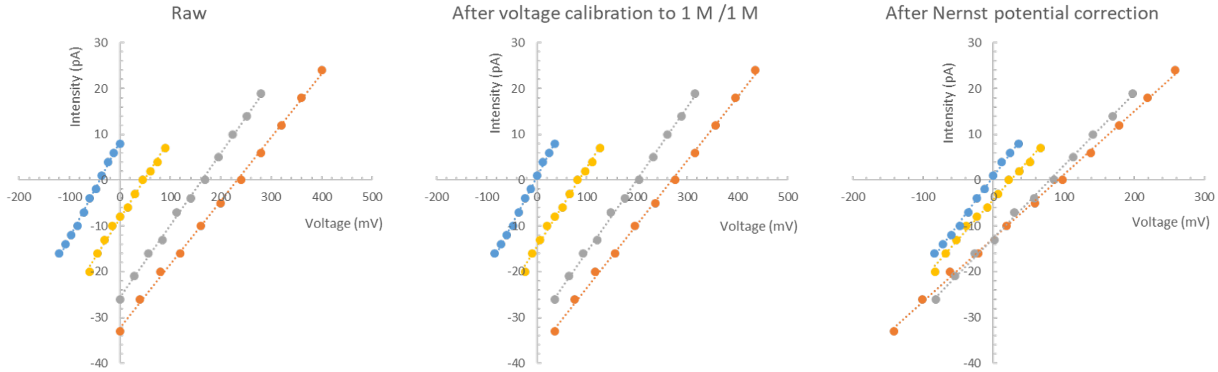

Figure S 5. Processing of reversal potential data (device Q1): raw data, after voltage calibration to 1 M / 1 M data (+ 36 mV), after Nernst potential correction (-59.13 mV per decade).

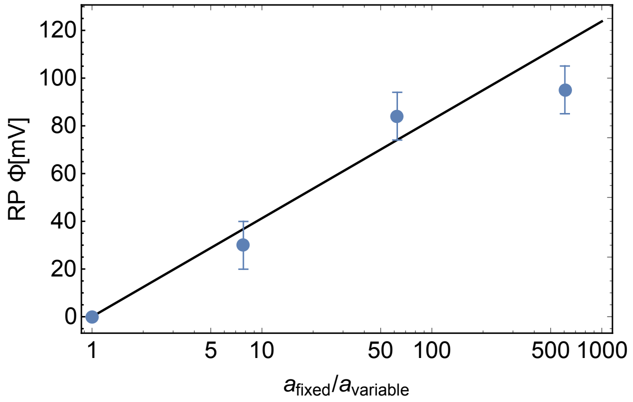

Figure S 6. Reversal potential fits using the Nernst equation (device Q1). The fitted ratio of transference numbers t+/t- is 5.7.

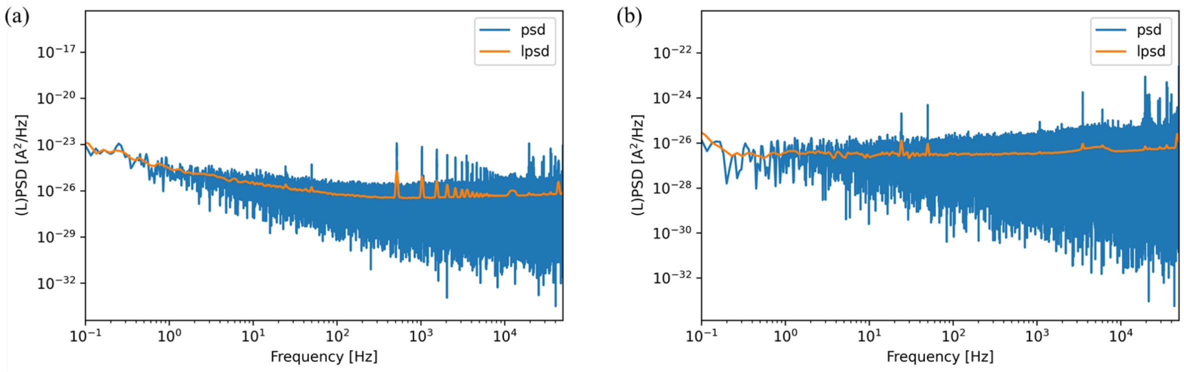

Figure S 7. PSD and LPSD of the same current traces showing the improved signal-to-noise ratio of LPSD. (a) V = + 1000 mV. (b) V = 0 mV.

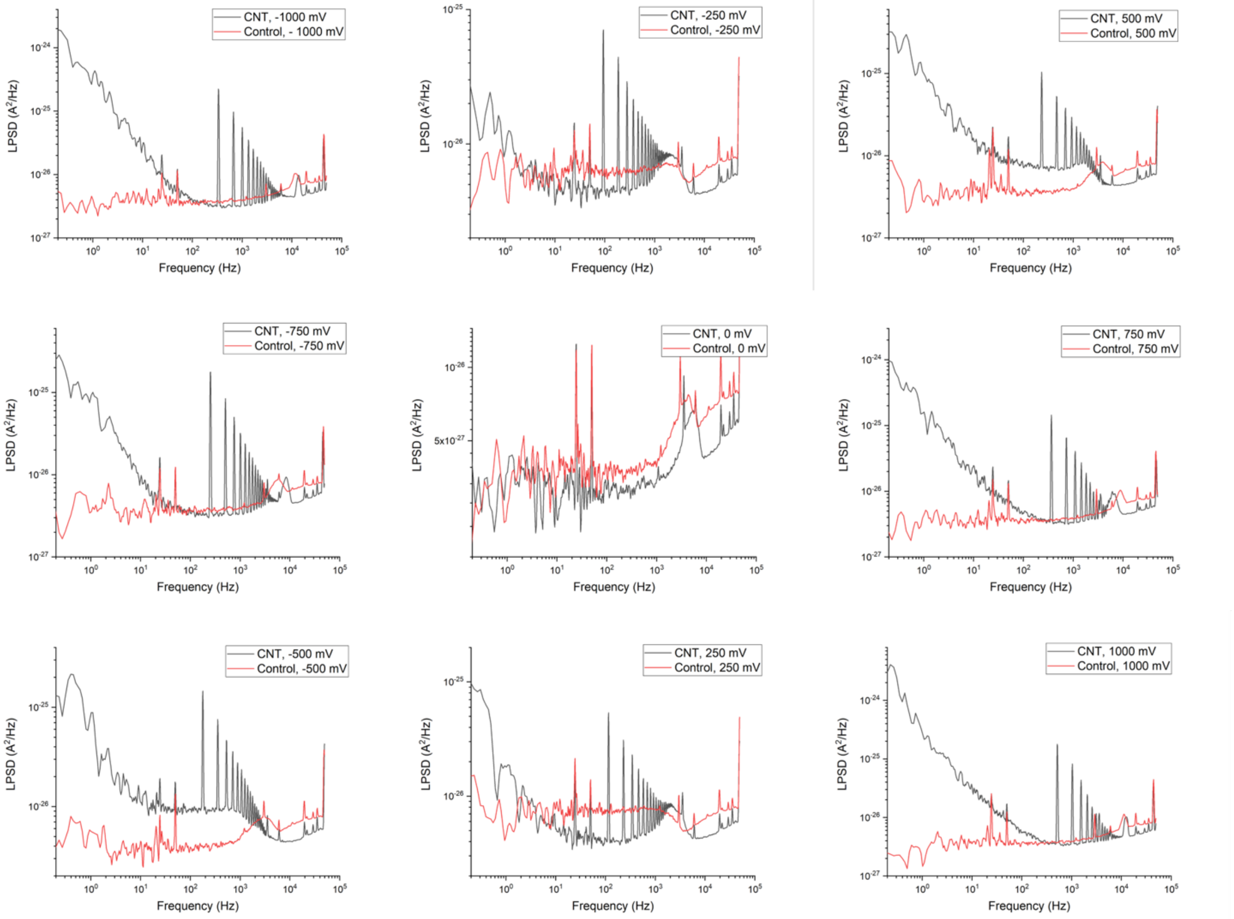

Figure S 8. LPSD of CNT and control for different applied voltages (device Q5, [KCl] = 10^{-2} M, pH = 10).

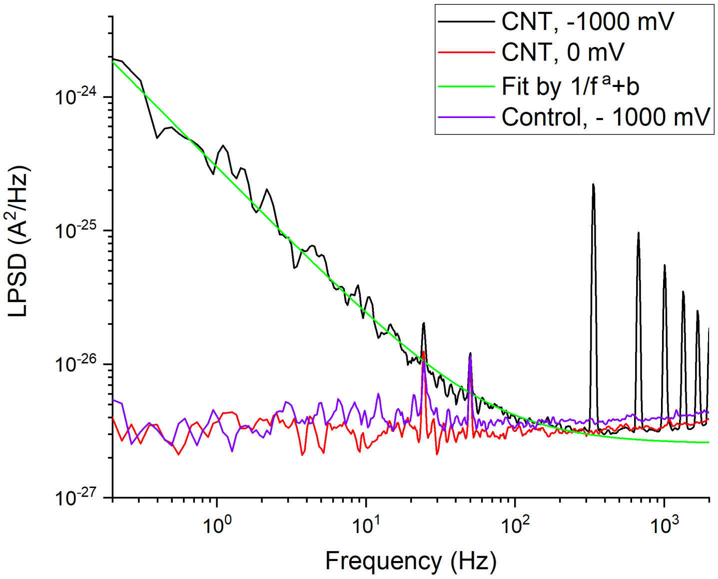

Figure S 9. LPSD of ionic current on CNT side at V=-1000 mV. The data for the control side at V=-1000 mV and for the CNT side at V = 0 V are also shown (device Q5, [KCl] = 10^{-2} M, pH = 10).

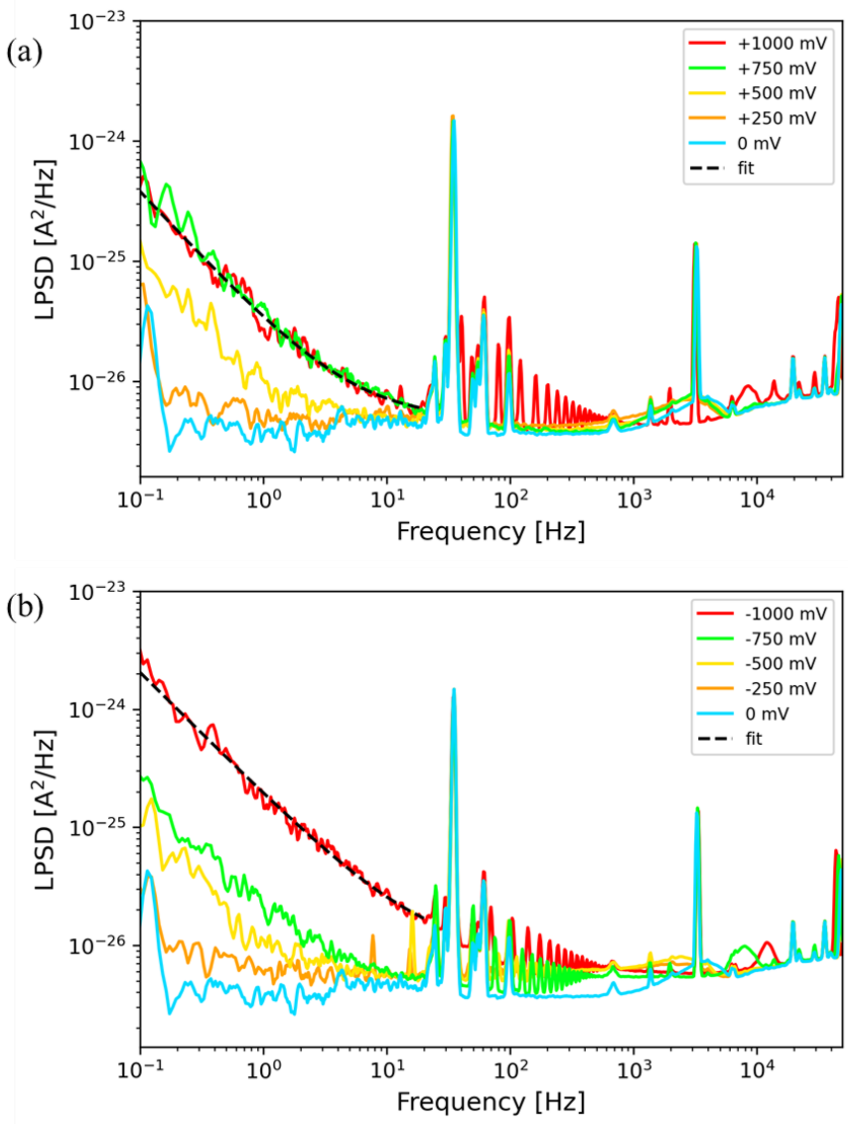

Figure S 10. LPSD of ionic current on CNT side at different voltages (device Q6, [KCl] = 10^{-2} M, pH = 7). From preliminary Raman characterization, this nanotube is a semiconducting SWCNT (resonant at 633 nm, non resonant at 532 nm and 785 nm) with a diameter of *ca* 2.0 nm (RBM at 126 cm^{-1}). The data at +/- 1000 mV were fitted in the low frequency range by $1/f^{a} + b$ with a = -1.10 and a = -1.04, respectively.

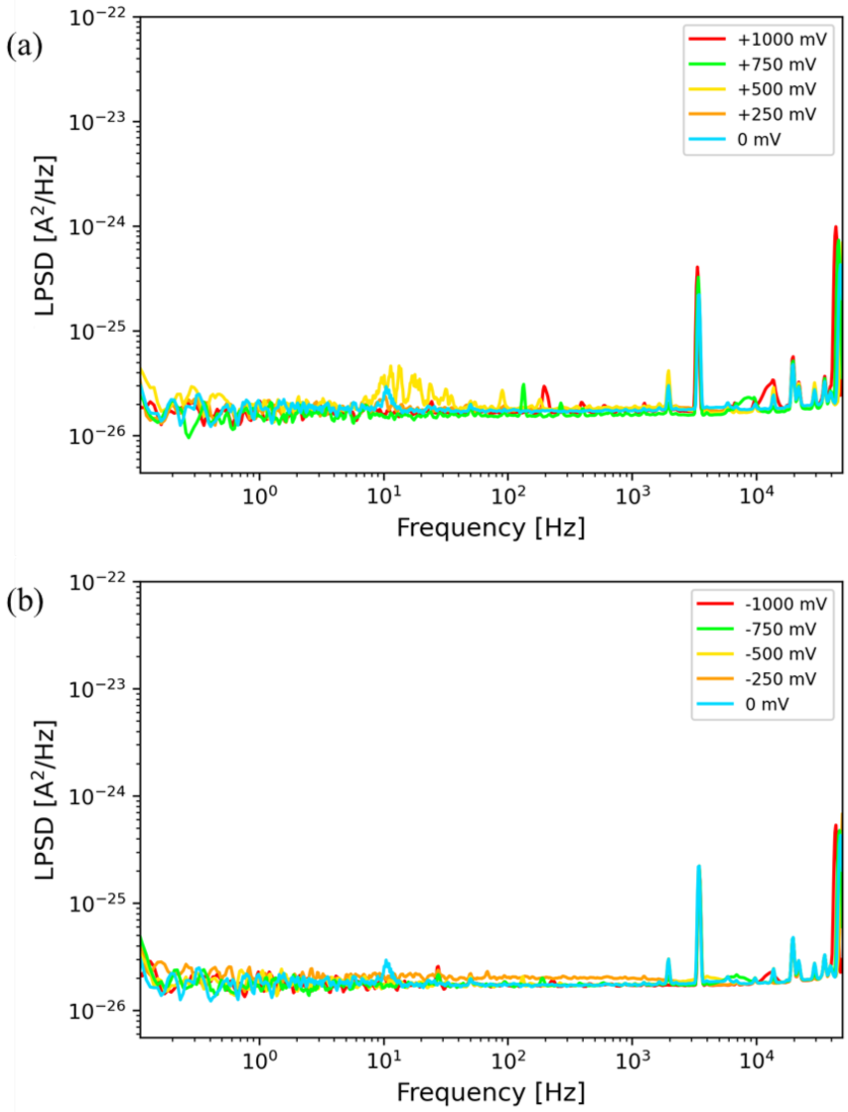

Figure S 11. LPSD of a quartz device without CNT, exhibiting a leak with conductance similar to that shown in Fig. S6 and measured under the same conditions ([KCl] = 1 M, pH = 5.5).

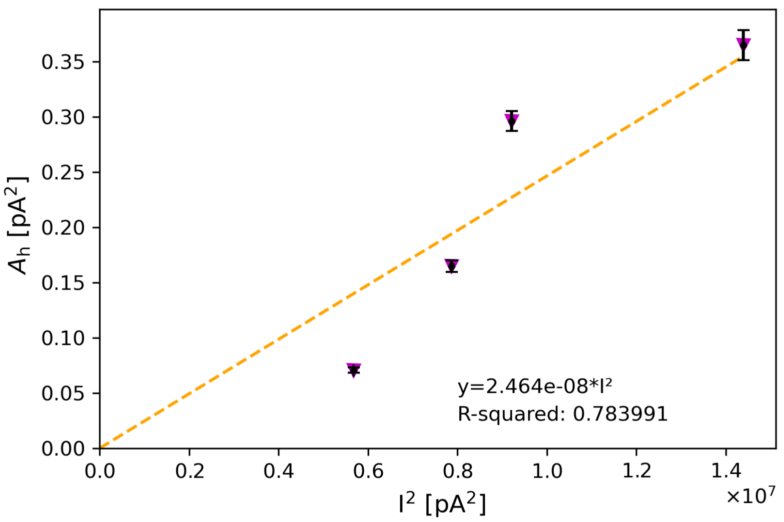

Figure S 12. A_H versus I^2 (device Q5, [KCl] = 10^{-2} M, pH = 10).

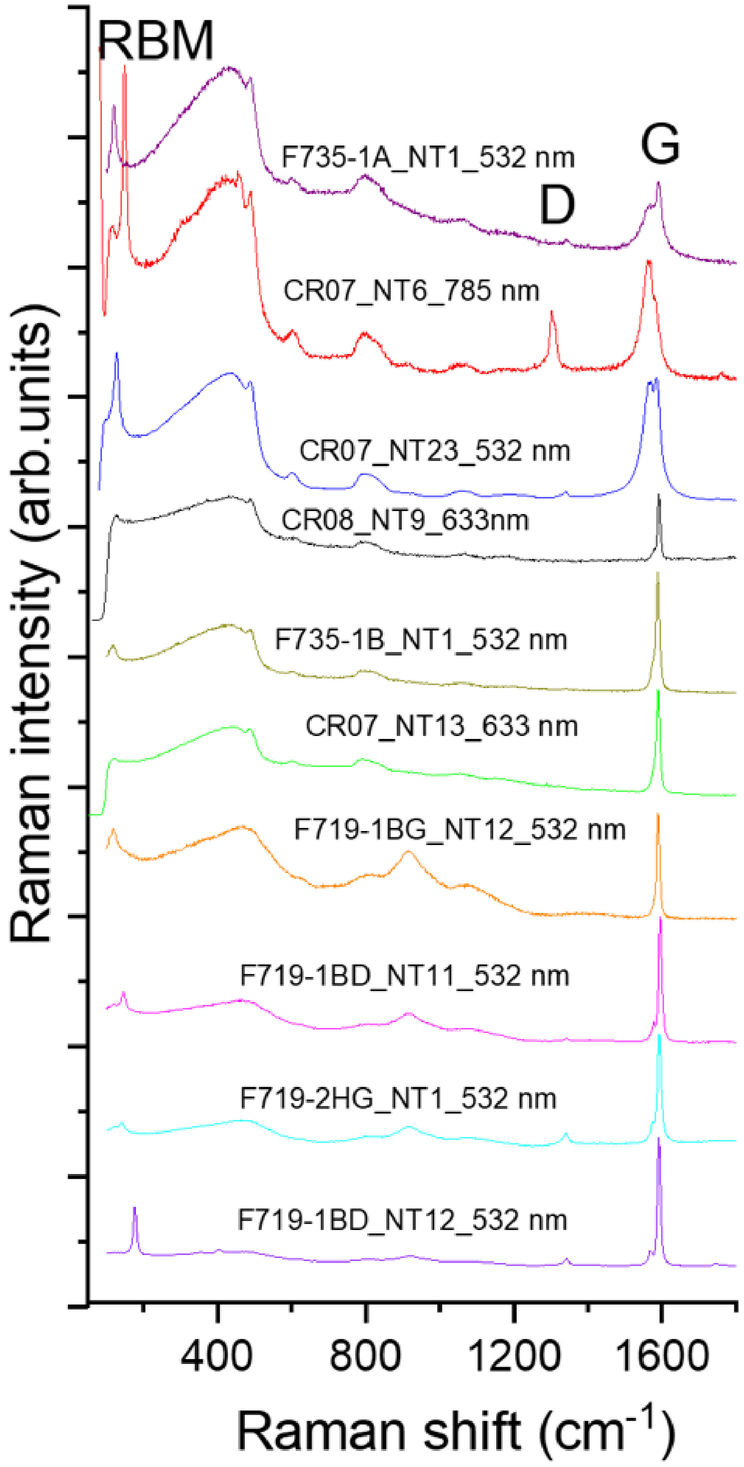

Figure S 13. Representative Raman spectra of individual nanotubes measured after growth and transfer to device substrates. As previously reported, the diameter range of SWCNTs in our samples is 1.2-2.0 nm (Yazda et al. (2017). Voltage-activated transport of ions through single-walled carbon nanotubes. Nanoscale, 9(33), 11976–11986). The broad bands between 300 cm^{-1} and 1200 cm^{-1} are photoluminescence bands of the SiO_2 substrate.

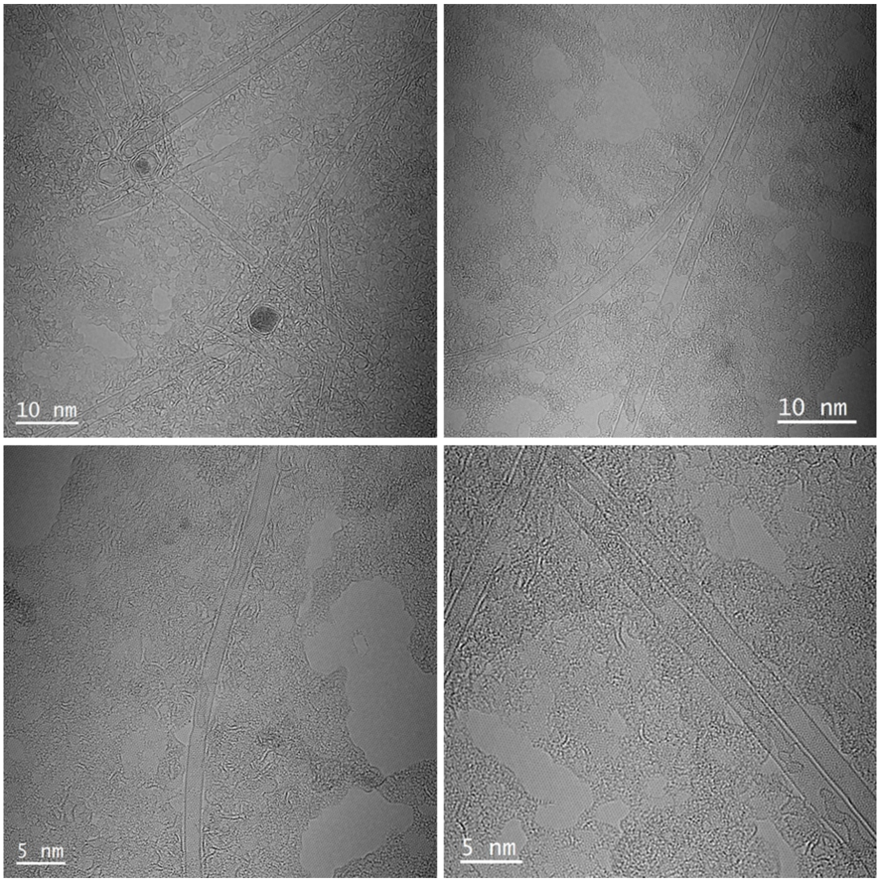

Figure S 14. High-resolution TEM performed on nanotubes grown in our group under close conditions (same substrate, catalyst, carbon precursor, and temperature but in another CVD reactor). The nanotubes were transferred from their growth substrate to TEM grids with a graphene monolayer as support. The TEM characterization showed a vast majority of SWCNTs with diameters between 1 and 3 nm, with few DWCNTs (clearly differentiable in the top left image) and no TWCNTs. Remains of the polymer (polystyrene) used for transferring the nanotubes to the TEM grid are also visible.